Bimodal phase percolation model for the structure of Ge-Se glasses and the existence of the intermediate phase

Pierre Lucas,[1] Ellyn A. King,[1,2] Ozgur Gulbiten,[1] Jeffery L. Yarger,[3] Emmanuel Soignard,[3] and Bruno Bureau[2]
[1]*Department of Materials Science and Engineering, University of Arizona, 4715 E. Fort Lowell Road, Tucson, Arizona 85712, USA*
[2]*UMR CNRS 6226 Sciences Chimiques, Groupe Verres et Céramiques, Université de Rennes I, Campus de Beaulieu, 35042 Rennes Cedex, France*
[3]*Department of Chemistry and Biochemistry, Arizona State University, Tempe, Arizona 85287-1604, USA*
(Received 19 October 2009; published 18 December 2009)

A detailed nuclear magnetic resonance and Raman study of Ge_xSe_{1-x} glasses indicate that the glass structure is composed of intertwined microdomains of $GeSe_2$ and Se_n. Static nuclear magnetic resonance spectra of glasses ranging from $0 \leq x \leq \frac{1}{3}$ reveal the absence of Ge-Se-Se fragments in the structure. High temperature nuclear magnetic resonance showing considerable line narrowing confirms this observation. More importantly, the fraction of Se-Se-Se obtained by integration of nuclear magnetic resonance lines matches closely the percentage predicted for a bimodal phase model and is not consistent with the existence of Ge-Se-Se fragments. Raman spectra collected on the same glass also confirm the existence of $GeSe_2$ domains up to high selenium concentrations. The mobility of the Se_n phase observed at high temperature while the $GeSe_2$ phase remains rigid is consistent with their respective underconstrained and overconstrained structural nature. The proposed bimodal phase percolation model is consistent with the original Phillips and Thorpe theory however it is clearly at odds with the intermediate phase model which predicts large amounts of Ge-Se-Se fragments in the structure. A calorimetric study performed over a wide range of cooling/heating rates shows a narrow composition dependence centered at $\langle r \rangle = 2.4$ in contrast with the wide reversibility window observed by Modulated Differential Scanning Calorimetry. This suggests that the observation of the reversibility window associated with the intermediate phase in Ge-Se glasses could be an experimental artifact resulting from the use of a single modulation frequency.

DOI: 10.1103/PhysRevB.80.214114 PACS number(s): 61.43.Dq, 81.05.Gc

I. INTRODUCTION

The structure of Ge_xSe_{1-x} glasses has long been a source of controversy in the field of amorphous semiconductors. The structure of Ge_xSe_{1-x} glasses in the range $0 \leq x \leq \frac{1}{3}$ was initially described using the chain crossing model (CCM), whereby $GeSe_{4/2}$ tetrahedra are linked by Se chains whose length increases with Se content.[1,2] However, this model was quickly contradicted by the persistent observation of a Raman line near 213 cm^{-1} associated with Ge-Se-Ge sequences[3] and later assigned to structural fragments composed of corner- and edge-sharing tetrahedra.[4,5] The presence of edge-sharing tetrahedra in Se-rich glasses is not consistent with the CCM and in particular contradicts the existence of an "ordered phase"[1] at $x=0.2$ ($GeSe_4$) where all Ge atoms would be linked by a Se-Se doublet. More recently, the structure of Ge_xSe_{1-x} has been the object of intense modeling efforts centered on topological arguments involving counting constraints and atomic degrees of freedom.[6–14] An original model by Phillips and Thorp predicts an optimal glass for an average number of bonds per atom $\langle r \rangle = 2.4$ corresponding to a topology where bond and angular constraints exactly equals the number of degrees of freedom in the structure.[6–8] This composition is characterized as the threshold between an underconstrained floppy phase for $\langle r \rangle < 2.4$ and an overconstrained rigid phase for $\langle r \rangle > 2.4$. The transition point $\langle r \rangle = 2.4$ is thought to correspond to the composition at which the rigid phase percolates throughout the structure. This model was later refined by invoking the "self-organization" of the glassy network which results in a structure that remains rigid but unstressed over a wider range of compositions near $\langle r \rangle = 2.4$.[15] The unstressed domain between the floppy and rigid phases was then termed the "intermediate phase." Subsequently, models based on connecting structural fragments of different connectivity were developed to rationalize the intermediate phase[11–14] and experimental measurements were performed to corroborate its existence.[10] In particular, the nonreversible enthalpy obtained by Modulated Differential Scanning Calorimetry (MDSC) was shown to decrease in this domain.[10] In any case it was found that the structural origin of the intermediate phase requires the existence of Se-Se-Ge "isostatic" structural fragments in order to account for the "rigid but unstressed" nature of the network.[12–14]

Among structural probes, solid state nuclear magnetic resonance constitutes a unique technique for examining the local environments of active elements in a qualitative and quantitative manner. But while silicate and phosphate glasses have been widely studied, chalcogenides and in particular selenides have received little attention due to the low nuclear magnetic resonance sensitivity of selenium.[16] Nevertheless, high quality spectra can be obtained using extended acquisition times up to several days.[17,18] In this work, an extensive high-temperature nuclear magnetic resonance study shows evidence for a different structural model of Ge-Se glasses based on a bimodal percolation of Se_n and $GeSe_2$ phases. It is shown that no significant amount of Se-Se-Ge fragments is present in the structure. These results are at odds with the existence of the intermediate phase. Calorimetric measurements on a series of Ge-Se glasses further suggest that the observation of the intermediate phase could be based on an experimental artifact.

II. EXPERIMENT

High-purity Ge_xSe_{1-x} glasses were synthesized using a high-vacuum procedure. 6N purity starting elements were introduced in a silica tube and further purified *in situ* by distilling high vapor pressure contaminants under a vacuum of 10^{-6} Torr. The silica tubes were subsequently sealed under vacuum and introduced into a rocking furnace for homogenization at 800 °C for 12 h. The melts were then quenched in water and annealed near Tg. The resulting rods were sliced into disks and the glass purity was monitored by Fourier transform infrared transmission.

Glass samples for nuclear magnetic resonance measurements were ground and introduced into an Avance 300 Bruker spectrometer. ^{77}Se nuclear magnetic resonance spectra were recorded from room temperature up to 520 °K in static mode. A Hahn spin echo sequence was applied and the whole echo was Fourier transformed in order to increase the signal to noise ratio and obtain some absorption mode line shape. The chemical shift was calibrated with a saturated solution of Me2Se in $CDCl_3$. Due to the low concentration and sensitivity of ^{77}Se, several thousand scans were accumulated and each spectrum was acquired over several days.

Raman spectra were acquired in a 180° geometry with a 785 nm laser source. The laser power was controlled using neutral density filters. The laser was focused onto the sample using a 20X long working distance Mitutoyo objective with a numerical aperture of 0.42. The signal was discriminated from the laser excitation light using a Kaiser supernotch filter followed with a Semrock edge filter. The data was collected using a Shamrock 303 Spectrograph and a deep depleted Andor charge coupled device detector. For each sample, spectra were first recorded at low intensity to ensure that no measurable changes due to photostructural effects took place during the measurement. The intensity and collection time were then progressively increased to optimize the signal to noise ratio while no visible spectral changes occurred.

Calorimetric measurements were performed with a Q1000 MDSC from TA Instruments. The glass transition temperature T_g was measured using a 10 °C/min cooling and heating rate. The activation energy for enthalpy relaxation was obtained following Moynihan's method.[19,20] Each sample was heated and equilibrated far above T_g then cooled far below T_g and reheated at the same rate. The procedure was repeated for rates ranging from 3 °C/min to 30 °C/min. The activation energy was estimated from the shift in T_g with heating rate. The whole sequence of measurements was performed on a series of eight Ge_xSe_{1-x} samples with average coordination ranging from $\langle r\rangle=2.2$ to $\langle r\rangle=2.55$. All measurements were performed in standard (nonmodulated) heating mode. The temperature was calibrated with an indium standard and the enthalpy was calibrated with a sapphire standard. Each sample was about 10–15 mg and held in a hermetic aluminum pan. An empty aluminum pan was used as a reference.

III. RESULTS

A. Nuclear magnetic resonance measurements

Room temperature nuclear magnetic resonance spectra of Ge_xSe_{1-x} glasses in the domain $0\leq x\leq\frac{1}{3}$ are presented in Fig. 1. The spectrum of pure selenium shows a single peak at 850 ppm consistent with the Se-Se-Se environment expected in selenium chains and rings. Likewise, the $GeSe_2$ spectrum shows one main peak at 430 ppm consistent with the Ge-Se-Ge environment expected in a structure composed of corner and edge sharing tetrahedra. More interestingly, it can be seen that the intermediate compositions $GeSe_4$ and $GeSe_9$ only display the same two peaks and do not show any additional signal associated with the Se-Se-Ge environment. By analogy with the As_xSe_{1-x} system,[21] this signal would be expected to appear approximately in between the two other peaks. However, the spectra can be properly fitted with only two lines as shown in Figs. 2(a) and 2(b). Reconstructed spectra using two simulated lines [Fig. 2(a)] result in a close fit with experimental data well within instrumental oscillations. Similarly, a reconstructed spectrum based on the addition of two scaled experimental lines from Se and $GeSe_2$ are shown in Fig. 2(b). While the fit is not optimum in some portion of the spectrum, the reconstruction shows that the experimental line position of Se and $GeSe_2$ exactly match the position of the lines present in $GeSe_4$.

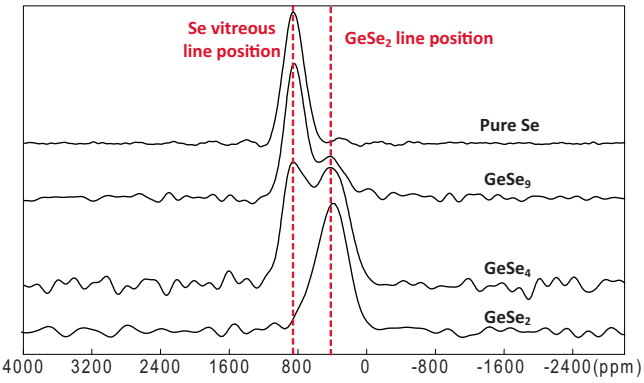

FIG. 1. (Color online) Experimental nuclear magnetic resonance ^{77}Se spectra of Se, $GeSe_9$, $GeSe_4$, and $GeSe_2$. Two types of line position are evidenced. The line near 850 ppm is attributed to Se connected to two neighboring Se as in pure vitreous Se. On the other hand, the line near 430 ppm is assigned to Se connected to two Ge as first neighbors as in $GeSe_2$.

Due to the broadness of the experimental nuclear magnetic resonance peaks, it is conceivable that an additional peak could be hidden between the two main lines observed in the room temperature spectra. In order to investigate this possibility, high-temperature nuclear magnetic resonance was performed on the Ge_xSe_{1-x} samples above their respective T_g. Increased structural mobility above T_g should result in line narrowing and help provide a greater resolution for the identification of experimental lines. Figure 3 shows the high temperature spectra of $GeSe_4$ up to 60 °K above T_g (experimental limitation). The series of spectra reveal a significant narrowing of the Se line with increasing temperature. On the other hand, the $GeSe_2$ does not exhibit a significant change in width. In order to quantify this effect, each spectra was fitted with simulated nuclear magnetic resonance lines as described in Fig. 2(a). The Se line was fitted with a Lorentzian shape (usually used for liquid state nuclear magnetic resonance), whereas the $GeSe_2$ was fitted with a Gaussian shape. Results of the fit are reported in Table I. The

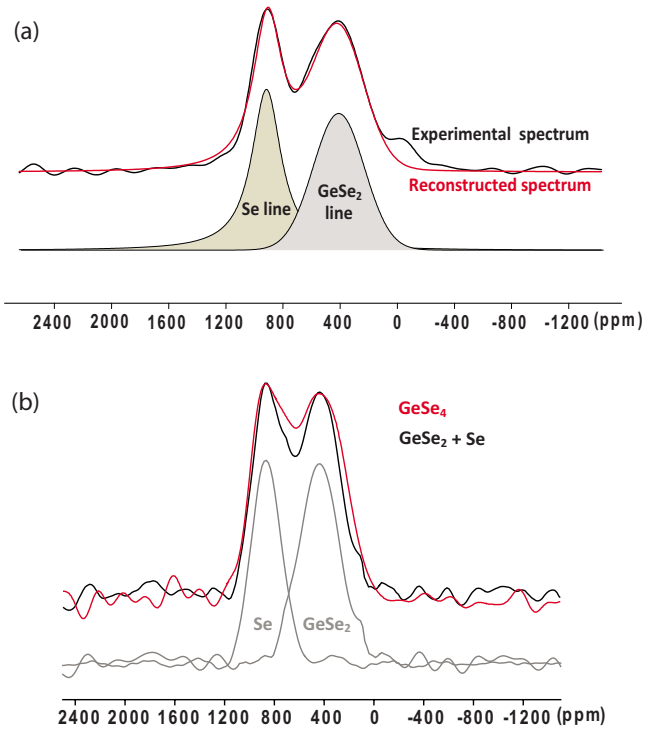

FIG. 2. (Color online) (a) Reconstruction of a ^{77}Se nuclear magnetic resonance static spectrum of $GeSe_4$ (540 °K) from simulated nuclear magnetic resonance lines. The Se type line is pure Lorentzian, whereas the $GeSe_2$ type line is strictly Gaussians. The reconstructed spectrum is superimposed with the experimental spectrum. (b) Reconstruction of a ^{77}Se nuclear magnetic resonance static spectrum of $GeSe_4$ from the experimental spectrum of pure Se and pure $GeSe_2$. The two experimental spectra were scaled in order to optimize the fit with the $GeSe_4$ spectrum. All spectra were acquired at room temperature.

fitting parameters confirm that the $GeSe_2$ line width does not vary significantly while the Se line continuously narrows with increasing temperature. This behavior is consistent with the increased mobility of Se chain fragments while the overconstrained $GeSe_2$ domains remain rigid. More importantly, it is shown that the integrated intensities of both peaks are equal within experimental error (±5%) at all temperatures.

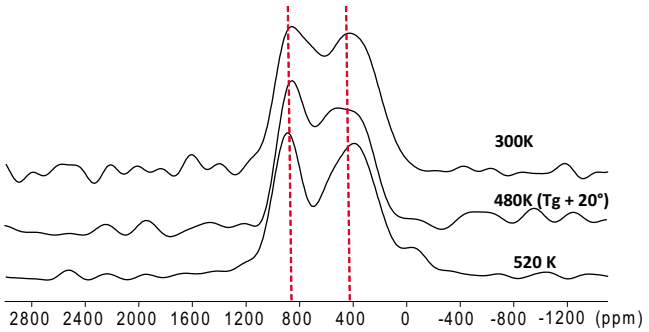

FIG. 3. (Color online) Nuclear magnetic resonance ^{77}Se spectra of $GeSe_4$ recorded at increasing temperature up to 60 °K above T_g (520 °K). The line narrowing results from thermally induced mobility in the structure. This narrowing is especially apparent for the Se line while the width of the $GeSe_2$ line stays mostly constant.

TABLE I. Parameters used for the reconstruction of the ^{77}Se nuclear magnetic resonance static spectra of $GeSe_4$ versus temperature. The Se type lines are pure Lorentzian, whereas the $GeSe_2$ type lines are strictly Gaussians. Each spectrum has been reconstructed using the DMFIT software.

	Lines	300 °K	460 °K	520 °K
Chemical shift (±10 ppm)	Se type line	840	860	890
	$GeSe_2$ type line	420	430	430
Integrated intensities (±5%)	Se type line	50	54	50
	$GeSe_2$ type line	50	46	50
Widths (±0.5 kHz)	Se type line	19	16	13
	$GeSe_2$ type line	24	24	23

This ratio of Se environments is indeed consistent with a description of $GeSe_4$ as composed of distinct microdomains of composition Se_2+$GeSe_2$ (50%Se-Se-Se+50%Ge-Se-Ge). It is worth noting that this structural model implies that no Ge-Se-Se sequence is present in the glass network. This description is, therefore, consistent with the spectra of Fig. 3, which show no significant additional peak associated with a Ge-Se-Se environment.

The same set of experiments performed on $GeSe_9$ further confirms this model. Due to the lower T_g of $GeSe_9$ it is possible to achieve higher structural mobility and considerable narrowing of the Se line. Figure 4 clearly shows that no significant Ge-Se-Se line appears upon narrowing of the Se-Se-Se peak. Due to the low nuclear magnetic resonance sen-

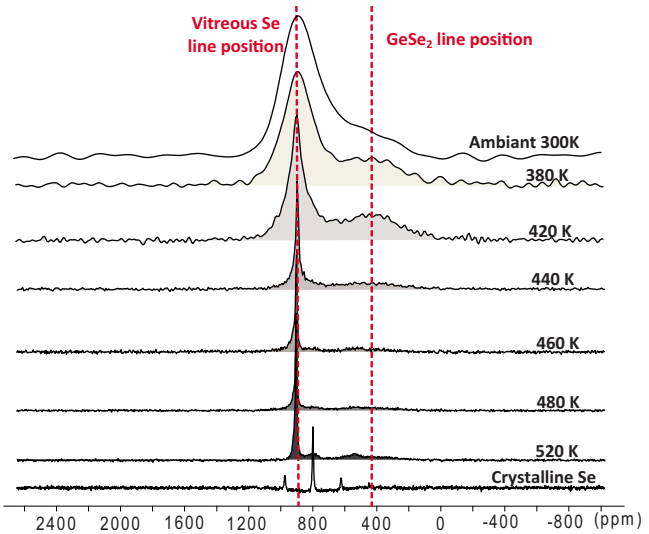

FIG. 4. (Color online) Nuclear magnetic resonance ^{77}Se spectra of $GeSe_9$ recorded at increasing temperature up to 150 °K above T_g. The Se line strongly narrows while the $GeSe_2$ line width remains constant. A third contribution appears at 520 °K (and slightly at lower temperature). This new line at 800 ppm is attributed to the crystalline phase of pure Se which appears due to the long holding time above T_g (acquisition time is more than 1 day for each spectrum).

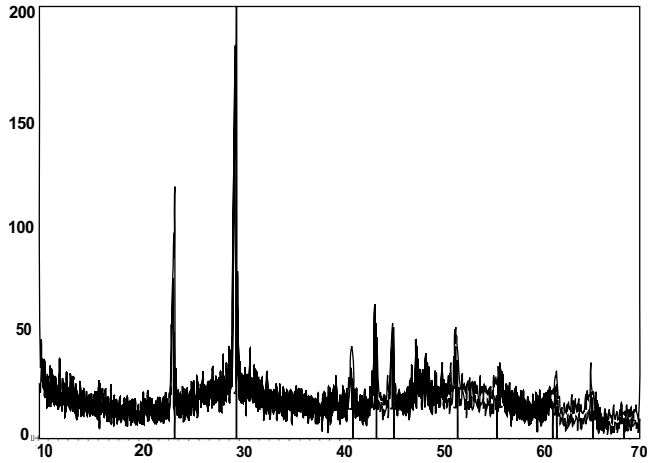

FIG. 5. XRD spectrum of a $GeSe_9$ sample after isothermal hold at 520 °K for more than a day. The markers correspond to the diffraction peak positions of crystalline selenium.

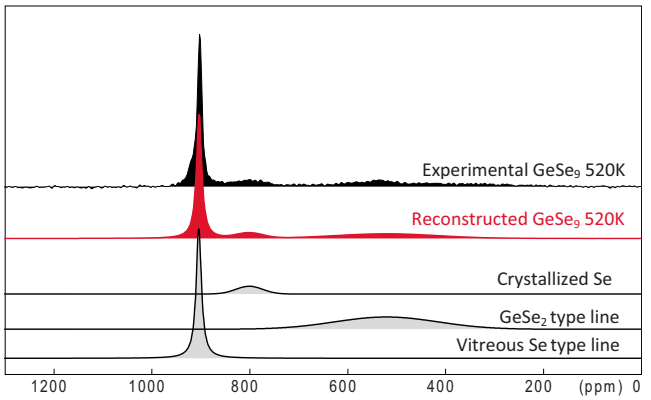

FIG. 6. (Color online) Experimental and reconstructed nuclear magnetic resonance ^{77}Se spectra of $GeSe_9$ at 520 °K. The parameters used for the reconstruction are listed in Table II. The $GeSe_2$ line and crystalline Se line are Gaussian while the mobile Se line is a Lorentzian.

sitivity of ^{77}Se, each spectrum must be collected for more than a day. As a consequence, some crystallization of selenium appears during isothermal holds at higher temperatures. The presence of crystalline selenium was indeed confirmed by x-ray diffraction performed on a sample held at 520 °K as shown in Fig. 5. The crystalline selenium line appears at 800 ppm on the nuclear magnetic resonance spectra as expected from the pure crystalline selenium data (Fig. 4). The high-temperature nuclear magnetic resonance spectra can then be reconstructed using three lines (pure Se, crystalline Se, and $GeSe_2$) as described in Fig. 6 for $GeSe_9$ at 520 °K. The same procedure was applied for all spectra and the fitting parameters are reported in Table II. Again, the main Se line undergoes a very notable sharpening with increasing temperature while the $GeSe_2$ line does not vary in width significantly. It is also noted that the nuclear magnetic resonance lines are shifted to higher ppm with increasing temperature. This shift is consistent with the temperature dependence of nuclear magnetic resonance line positions, but might also be associated with the onset of structural degradation. More importantly, it is shown that the relative intensity of Se lines to $GeSe_2$ line is approximately constant for all temperatures (within experimental error). Moreover, the experimental percentages reported at ~75%Se-Se-Se and ~25%Se-Ge-Se environments is very consistent with a description of $GeSe_9$ as composed of distinct microdomains of composition Se_7+GeSe_2 (78%Se-Se-Se+22%Ge-Se-Ge). Again, this model implies the absence of Ge-Se-Se lines in agreement with the experimental spectra.

B. Raman spectra

Raman spectra of Ge_xSe_{1-x} glasses display three main lines centered at 195 cm^{-1}, 213 cm^{-1}, and 255 cm^{-1}. The line at 255 cm^{-1} is assigned to Se chain modes and can be fitted with three Gaussians, while the lines at 195 and 213 cm^{-1} can each be fitted with a single Gaussian and are, respectively, assigned to corner-sharing and edge-sharing tetrahedral breathing modes [Fig. 7(a)]. It can be shown that the intensity of Se chain modes decreases with increasing x

TABLE II. Parameters used for the reconstruction of the ^{77}Se nuclear magnetic resonance static spectra of $GeSe_9$ versus temperature. The amorphous Se type lines are pure Lorentzian, while the crystalline Se and $GeSe_2$ lines are Gaussians. Each spectrum has been reconstructed using the DMFIT software.

	Line	300 K	380 K	420 K	440 K	460 K	480 K	520 K
Chemical shift	Se type line (±1 ppm)	870	875	877	893	898	900	905
	$GeSe_2$ type line (±10 ppm)	440	440	440	460	480	510	540
	Crystallized Se (±5 ppm)				790	790	790	790
Integrated intensities (±5%)	Se type line	80	75	75	75	70	67	61
	$GeSe_2$ type line	20	25	25	25	25	28	29
	Crystallized Se					5	5	10
Widths	Se type line ±0.5 kHz	15.7	13.2	6.7	1.5	1.0	0.9	0.7
	$GeSe_2$ type line ±2 kHz	22	21	21	22	23	22	15
	Crystallized Se ±0.5 kHz				4.5	4	5	4

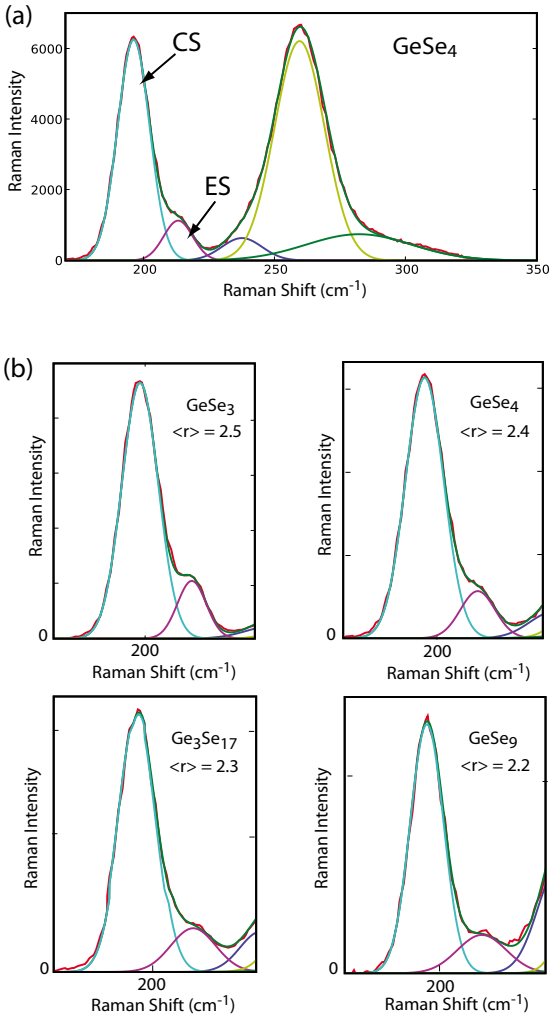

FIG. 7. (Color online) (a) Raman spectra of $GeSe_4$ deconvoluted with 5 Gaussian peaks: 1 for corner-sharing tetrahedral mode (CS), 1 for edge-sharing tetrahedral modes (ES) and 3 for the selenium chain modes. (b) Tetrahedral modes of Ge_xSe_{1-x} glasses with $\langle r \rangle = 2.2-2.4$.

while the intensity of tetrahedral modes increases. More interestingly, it can be noted that the edge-sharing mode intensity is still substantial even at high Se concentrations. The persistence of this mode is made clearly visible by normalizing the tetrahedral peaks of Ge_xSe_{1-x} samples ranging from $x=0.33$ down to 0.1 as illustrated in Fig. 7(b). This implies that $GeSe_{4/2}$ tetrahedra tend to aggregate together even when they are dissolved into large fraction of selenium. The presence of this mode is usually associated with structural fragments reminiscent of crystalline $GeSe_2$ composed of chains of corner-sharing tetrahedra linked by edge-sharing tetrahedra.[4] The observation of this mode is therefore quite consistent with the structural model derived from the nuclear magnetic resonance data. Furthermore, an integration of edge- and corner-sharing peaks over the whole composition range shows that the variation in corner/edge ratio is surprisingly small even though the Se/Ge ratio increases from 3 to 10 (see Table III). This confirms that $GeSe_{4/2}$ tetrahedra remain aggregated upon dilution into fractions of selenium as large as Se/Ge=1/10 where all tetrahedra could be separated

TABLE III. Raman intensity ratio of corner-sharing to edge-sharing tetrahedral modes in Ge_xSe_{1-x} glasses with $\langle r \rangle = 2.2-2.5$. The ratios were obtained by integration of the fitted Gaussian peaks for each compositions.

Ratio Corner/Edge	$\langle r \rangle$	Se/Ge
4.43	2.5	3
5.53	2.4	4
5.89	2.3	5.7
6.50	2.2	10

from each other by selenium chains more than four units long if they followed the CCM model. The Raman data are, therefore, fully consistent with the nuclear magnetic resonance results and while the Raman does not specifically dismiss the existence of Ge-Se-Se fragments, it clearly supports a model based on two microphases of $GeSe_2$ and Se_n.

C. Calorimetric study

The existence of Ge-Se-Se fragments in Ge_xSe_{1-x} glasses near $\langle r \rangle = 2.4$ is believed to result in rigid but unstressed networks that have unusual physical properties such as the absence of nonreversing enthalpy at T_g. These enthalpy measurements are typically performed with MDSC using a single temperature oscillation frequency superimposed on the normal heating rate. One potential concern with this measurement is that glasses relax with a wide spectrum of relaxation times and consequently a single oscillation frequency might only capture parts of the relaxation process. In contrast, measurements of the activation energy for enthalpy relaxation (E_A) are performed using a set of cooling/heating rates ranging from 3 °C/min to 30 °C/min. These measurements, therefore, permit the probing of the glass relaxation with time constants extending over one order of magnitude. Figure 8 describes the result of such a measurement for a Ge_3Se_{17} sample. The experimental values of $1000/T_g$ show a linear dependence on the natural log of the cooling rate lnQ and the slope of the resulting plot yields the activation en-

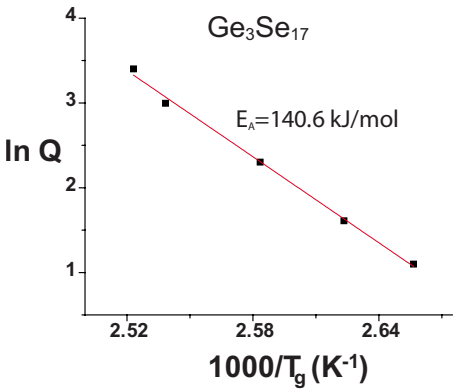

FIG. 8. (Color online) Plot of the shift in T_g when measured at different cooling/heating rates Q. The slop of the lnQ vs $1000/T_g$ plot is equal to E_A/R where R is the gas constant and E_A is the activation energy for enthalpy relaxation.

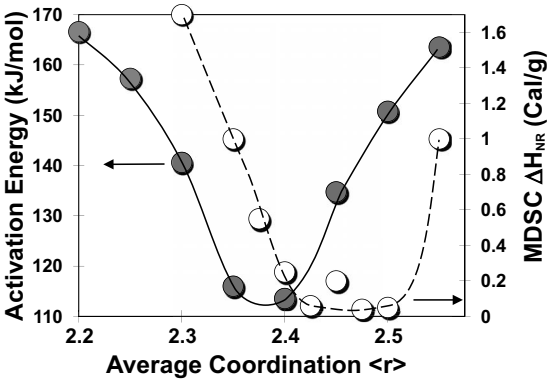

FIG. 9. Activation energy for enthalpy relaxation measured by the cooling rate method described in Fig. 8 for a series of Ge_xSe_{1-x} glasses ranging from $\langle r\rangle=2.2$ to 2.55. For comparison, the white dots represent the nonreversible enthalpy measured by MDSC (Ref. 24).

ergy E_A. Systematic measurements of E_A for a set of glass samples ranging from $\langle r\rangle=2.2$ to 2.55 are reported in Fig. 9 and compared with the nonreversible enthalpy ΔH_{NR} measured by MDSC on equivalent samples. The variation in E_A shows a single minimum near $\langle r\rangle=2.4$ in agreements with the original model of Phillips and Thorpe for rigidity percolation. These results contrast with the MDSC measurements which yields a wide nonreversibility window from $\langle r\rangle=2.4$ to 2.5. The single minima observed here is expected to result from the percolation of a rigid phase though a floppy phase at $\langle r\rangle=2.4$.[6] This behavior is therefore consistent with the bimodal phase structure derived from nuclear magnetic resonance and Raman. Indeed, the $GeSe_2$ domains are overconstrained and rigid while the Se_n domains are underconstrained and floppy. The $GeSe_2$ domains, therefore, appear to percolate through the structure into a continuous network at $\langle r\rangle=2.4$. Meanwhile, the intermediate phase proposed as the structural basis for the nonreversing window requires the existence of Ge-Se-Se fragments which are not observed by nuclear magnetic resonance. This might suggest that the observation of a nonreversing window in Ge_xSe_{1-x} glasses could be an experimental artifact resulting from the limitation of the MDSC measurement at a single oscillation frequency.

IV. DISCUSSION

A. Bimodal phase model

Solid state nuclear magnetic resonance has long been accepted as a powerful tool for resolving the structure of glassy materials. In that respect, nuclear magnetic resonance studies of As_xSe_{1-x} are fully consistent with a structural model based on $AsSe_{3/2}$ pyramids linked by Se chain fragments.[16,21] Three distinct Se environments can be clearly resolved at 850ppm for Se-Se-Se, 550ppm for As-Se-Se and 380ppm for As-Se-As, in agreement with the chain crossing model. Arsenic and germanium being neighbors in the periodic table means that they have very similar electronegativities and form similar covalent bonds with selenium. It is therefore expected that the nuclear magnetic resonance response of Ge_xSe_{1-x} glasses should be relatively analogous if they also adopt the chain crossing structural model. However, results from this study show very clearly otherwise. Only two Se environments are present in Se-rich Ge_xSe_{1-x} glasses which can be unambiguously assigned to the Se-Se-Se environment present in pure selenium and to the Ge-Se-Ge environment present in pure $GeSe_2$. This striking contrast to the nuclear magnetic resonance of As_xSe_{1-x} implies that the Ge_xSe_{1-x} glass structure is not based on $GeSe_{4/2}$ tetrahedra cross-linked by Se chains because this model would require large amounts of Ge-Se-Se environments well above the detection limit of nuclear magnetic resonance spectrometry. Accordingly, the glass structure must not involve significant amounts of Ge-Se-Se sequences and it can easily be shown that the only structural model that can satisfy this requirement and match the nuclear magnetic resonance spectra is based on the percolation of two phases of $GeSe_2$ and Se_n.

The second and more crucial observation derived from the nuclear magnetic resonance data is that the measured fraction of Se-Se-Se closely matches that predicted from the bimodal phase model. This implies that the remaining fraction of Se must be in a Ge-Se-Ge environment in order to satisfy the valence of Ge and the glass stoichiometry. As a consequence, the Se-Se-Se peak integration effectively implies that no significant amount of Ge-Se-Se can be present in the structure. It must be noted that this derivation is only true in the absence of large amounts of Ge-Ge homopolar bonds in the structure. This provision is confirmed by the Raman analysis which shows no Se_3Ge-$GeSe_3$ modes at 178 cm^{-1} for any of the compositions studied. Finally, the above discussion is strongly reinforced by the high-temperature nuclear magnetic resonance spectra because the narrowing of the line at 850 ppm unambiguously confirms its assignment to the Se-Se-Se environment while the increased resolution corroborates the absence of a Ge-Se-Se peak. Furthermore, the experimentally measured Se-Se-Se fraction remains in close agreement with the bimodal phase model at all temperatures for both compositions studied. Hence, both peak position and peak integration concur and lead to a model of bimodal phase percolation based on $GeSe_2$ and Se_n domains.

A third observation from the high-temperature nuclear magnetic resonance spectra also indirectly supports the proposed structural model. The considerable narrowing of the Se-Se-Se line is indicative of increased mobility of Se atoms in this phase. This is quite consistent with the structural flexibility expected from the floppiness of Se_n phase. Meanwhile, the width of the Ge-Se-Ge line remains unchanged at higher temperature, which is also consistent with the rigidity expected from the over-constrained $GeSe_2$ phase. Hence, the glass structure can be sensibly described as two intimately intertwined phases linked only by Van der Waals interactions but not covalently bonded to each other as illustrated in Fig. 10.

The Raman analysis of these glasses also supports the bimodal phase model through the observation of a significant and persistent edge-sharing tetrathedral mode at 213 cm^{-1}. While the precise origin of this mode has been the subject of controversies,[3–5,10] it is unambiguously associated with $GeSe_2$-like fragments of clustered tetrahedra. The presence

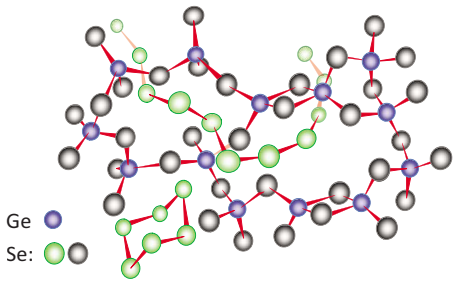

FIG. 10. (Color online) Schematic representation of the structure of Ge_xSe_{1-x} glasses following the bimodal phase model based on intertwined domains of $GeSe_2$ and Se_n. The two domains are linked by Van der Waals interactions but are not covalently bonded. Se atom in the $GeSe_2$ phase atoms and Se atoms in the Se_n phase are represented in different colors.

of aggregated tetrahedra for Ge/Se ratio as large as 1/10 therefore corroborates a two phase model.

B. Intermediate phase model

The concept of the intermediate phase (IP) was originally suggested by Phillips and Thorp as a finite compositional domain where the glass network is rigid but unstressed.[15] Two types of theoretical models have been proposed to advocate for the IP in the Ge-Se system, a model based on a constraint counting algorithm[11,12] and a model based on a computer generated network of nodal atoms.[14] The core of both of these models rely on the presence of a high concentration of Se-Se-Ge isostatic structural fragments in order to account for the "rigid but unstressed" nature of the network, i.e., the network optimizes the chain length between nodal Ge atoms such as to minimize local stress. Nevertheless, while the IP has received a lot of theoretical support[11–15,22] the present experimental data appear to conflict with this model, i.e., the distribution of Se environments observed experimentally widely differs from that predicted by the IP. An example is shown in Fig. 11 for the standard $GeSe_4$ composition. The fraction of Se environments derived from nuclear magnetic resonance data is compared with that predicted from the bimodal phase model, the chain crossing model[1] and the IP.[13] It is shown that the bimodal phase model closely matches the experimental data while the chain crossing model and the IP model widely differs. In particular, the IP model predicts 47% of Se-Se-Ge environments while the nuclear magnetic resonance data does not detect such environment within the experimental error of ~5%.

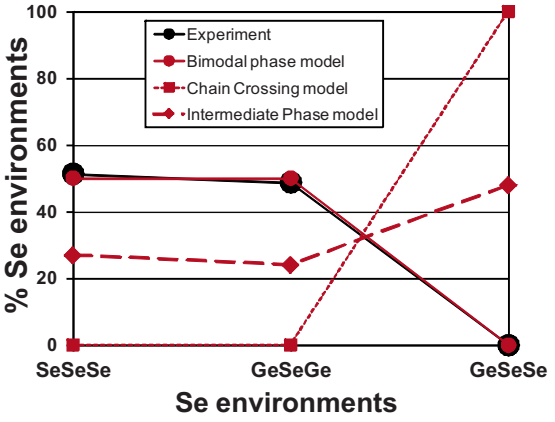

FIG. 11. (Color online) Relative percentage of the three possible selenium environments in $GeSe_4$ according to the intermediate phase model (Ref. 13), the chain crossing model (Ref. 1), and the bimodal phase model proposed here and compared with experimental percentage obtained by nuclear magnetic resonance.

Other experimental measurements based on x-ray diffraction have shown to be consistent with the IP (Ref. 22), however, a recent comparison of first principle structural models with neutron and x-ray diffraction data on $GeSe_2$ glass concluded that diffraction probes are not sufficiently selective to differentiate between a structural model derived from chemical order and a structural model with a high degree of chemical disorder.[23] Indeed, these results are consistent with some recent high resolution synchrotron and extended x-ray absorption fine structure data that could not identify any structural discontinuity in the region proposed for the IP.[24] The other experimental measurement that is most often invoked to support the IP is based on quantifying the nonreversible enthalpy by MDSC.[10,24–26] However, that measurement might also be subjected to a large experimental uncertainty. Since the seminal crossover experiments of Napolitano and co-workers,[27–29] it is well understood that glass relaxation involves a wide spectrum of relaxation times. Some structural domains in the glass relax quickly while some others relax slowly. It was recently demonstrated that this phenomenon is associated with density fluctuations in the glass structure.[30] Usually, the shape of the relaxation time spectrum is conveniently described using a single parameter β that quantifies the nonexponential character of the relaxation function.[31–33] It was shown that the magnitude of β varies significantly with composition[34,35] as well as the fictive temperature[36,37] of a glass. In particular, it is known to vary significantly with $\langle r \rangle$ in chalcogenide glass systems.[38] Nevertheless, MDSC experiments are typically performed at a single modulation frequency of 100 s, which is more or less equal to the medium relaxation time of a glass at T_g. This implies that such an MDSC experiment might not capture the slower relaxation processes during measurements of the nonreversible enthalpy. Hence, if only a fraction of the distribution of relaxation times is captured while this distribution changes with $\langle r \rangle$, there is a large potential for uncertainty in the measurement of the reversibility window associated with the IP. On the other hand, a parallel calorimetric measurement involving a wide range of time scales such as the determination of the activation energy shows a narrow composition dependence centered at $\langle r \rangle = 2.4$ in contrast with the wider window observed by MDSC. This discrepancy suggests that the observation of the reversibility window might be associated with an experimental artifact due to the use of a single modulation frequency.

V. CONCLUSIONS

In covalent network glasses such as chalcogenides, it is well understood that the local building blocks are based on

the element valence, i.e., chains for divalent Se, trigonal pyramids for trivalent As or tetrahedra for tetravalent Ge. However, the extended connection between these building blocks is still the subject of much controversy, yet it is of fundamental importance since it largely controls the physical properties of the glass. It is shown that direct structural probes such as nuclear magnetic resonance and Raman lead to a structural description of Ge-Se glasses based on a bimodal phase percolation of $GeSe_2$ and Se_n domains. This structural model is derived from multiple experimental observations including: (i) only two ^{77}Se lines for the Se-Se-Se and Ge-Se-Ge environments (but no Ge-Se-Se) are found by nuclear magnetic resonance even at high temperature where lines narrows considerably, (ii) the population of Se-Se-Se obtained by integration of nuclear magnetic resonance peaks is only consistent with a two phase model and corroborates the absence of Ge-Se-Se fragments, (iii) high T nuclear magnetic resonance shows that the Se_n phase is mobile while the $GeSe_2$ phase is rigid at high temperature in agreement with their respective expected structural rigidity, (iv) the Raman spectra are consistent with the presence of a rigid $GeSe_2$ phase even at high Se content. These results are at odds with the existence of the IP in the Ge-Se system. Calorimetric measurements performed over a wide range of cooling rates suggest that the observation of the reversibility window might be an experimental artifact.

ACKNOWLEDGMENT

This work was supported by NSF-DMR under Grant No. 0806333, and the CNRS International Associated Laboratory, Materials & Optics. J.Y. and E.S. acknowledge support from the National Nuclear Security administration Carnegie/DOE Alliance Center (NNSA CDAC).

[1] P. Tronc, M. Bensoussan, A. Brenac, and C. Sebenne, Phys. Rev. B **8**, 5947 (1973).
[2] G. J. Ball and J. M. Chamberlain, J. Non-Cryst. Solids **29**, 239 (1978).
[3] R. J. Nemanich, S. A. Solin, and G. Lucovsky, Solid State Commun. **21**, 273 (1977).
[4] P. M. Bridenbaugh, G. P. Espinosa, J. E. Griffiths, J. C. Phillips, and J. P. Remeika, Phys. Rev. B **20**, 4140 (1979).
[5] K. Murase, K. Yakushiji, and T. Fukunaga, J. Non-Cryst. Solids **59-60**, 855 (1983).
[6] M. F. Thorpe, J. Non-Cryst. Solids **57**, 355 (1983).
[7] H. He and M. F. Thorpe, Phys. Rev. Lett. **54**, 2107 (1985).
[8] J. C. Phillips, J. Non-Cryst. Solids **34**, 153 (1979).
[9] X. Feng, W. J. Bresser, and P. Boolchand, Phys. Rev. Lett. **78**, 4422 (1997).
[10] P. Boolchand, X. Feng, and W. J. Bresser, J. Non-Cryst. Solids **293-295**, 348 (2001).
[11] M. Micoulaut, EPL **58**, 830 (2002).
[12] M. Micoulaut and J. C. Phillips, Phys. Rev. B **67**, 104204 (2003).
[13] C. Massobrio, M. Celino, P. S. Salmon, R. A. Martin, M. Micoulaut, and A. Pasquarello, Phys. Rev. B **79**, 174201 (2009).
[14] A. Sartbaeva, S. A. Wells, A. Huerta, and M. F. Thorpe, Phys. Rev. B **75**, 224204 (2007).
[15] M. F. Thorpe, D. J. Jacobs, M. V. Chubynsky, and J. C. Phillips, J. Non-Cryst. Solids **266-269**, 859 (2000).
[16] C. Rosenhahn, S. E. Hayes, B. Rosenhahn, and H. Heckert, J. Non-Cryst. Solids **284**, 1 (2001).
[17] B. Bureau, J. Troles, M. Le Floch, P. Guenot, F. Smektala, and J. Lucas, J. Non-Cryst. Solids **319**, 145 (2003).
[18] B. Bureau, J. Troles, M. Le Floch, F. Smektala, and J. Lucas, J. Non-Cryst. Solids **326-327**, 58 (2003).
[19] C. T. Moynihan, A. J. Easteal, M. A. DeBolt, and J. Tucker, J. Am. Ceram. Soc. **59**, 12 (1976).
[20] C. T. Moynihan, S. K. Lee, M. Tatsumisago, and T. Minami, Thermochim. Acta **280-281**, 153 (1996).
[21] B. Bureau, J. Troles, M. LeFloch, F. Smektala, G. Silly, and J. Lucas, Solid State Sci. **5**, 219 (2003).
[22] F. Inam, M. T. Shatnawi, D. Tafen, S. J. L. Billinge, P. Chen, and D. A. Drabold, J. Phys.: Condens. Matter **19**, 455206 (2007).
[23] L. Giacomazzi, C. Massobrio, and A. Pasquarello, Phys. Rev. B **75**, 174207 (2007).
[24] M. T. M. Shatnawi, C. L. Farrow, P. Chen, P. Boolchand, A. Sartbaeva, M. F. Thorpe, and S. J. L. Billinge, Phys. Rev. B **77**, 094134 (2008).
[25] P. Boolchand, D. G. Georgiev, and B. Goodman, J. Optoelectron. Adv. Mater. **3**, 703 (2001).
[26] S. Chakravarty, D. G. Georgiev, P. Boolchand, and M. Micoulaut, J. Phys.: Condens. Matter **17**, L1 (2005).
[27] A. Napolitano and P. B. Macedo, J. Res. Natl. Bur. Stand., Sect. A **72**, 425 (1968).
[28] L. Boesch, A. Napolitano, and P. B. Macedo, Am. Ceram. Soc. Bull. **47**, 405 (1968).
[29] L. Boesch, A. Napolitano, and P. B. Macedo, J. Am. Ceram. Soc. **53**, 148 (1970).
[30] J. C. Mauro, S. S. Uzun, W. Bras, and S. Sen, Phys. Rev. Lett. **102**, 155506 (2009).
[31] C. T. Moynihan *et al.*, Ann. N. Y. Acad. Sci. **279**, 15 (1976).
[32] G. W. Scherer, J. Non-Cryst. Solids **123**, 75 (1990).
[33] I. M. Hodge, Science **267**, 1945 (1995).
[34] R. Böhmer, K. L. Ngai, C. A. Angell, and D. J. Plazek, J. Chem. Phys. **99**, 4201 (1993).
[35] I. M. Hodge, J. Non-Cryst. Solids **169**, 211 (1994).
[36] G. W. Scherer, J. Am. Ceram. Soc. **69**, 374 (1986).
[37] R. Böhmer and C. A. Angell, Phys. Rev. B **48**, 5857 (1993).
[38] R. Böhmer and C. A. Angell, Phys. Rev. B **45**, 10091 (1992).